

## Accepted Manuscript

Evolution of Physical and Photocatalytic Properties of New Zn(II) and Ru(II) complexes

Venkanna Gugulothu, Jakeer Ahemed, Mahesh Subburu, Bhongiri Yadagiri, Ritu Mittal, Chetti Prabhakar, Someshwar Pola

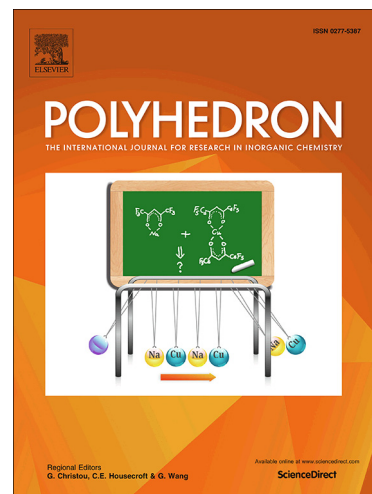
PII: S0277-5387(19)30403-6  
DOI: <https://doi.org/10.1016/j.poly.2019.05.065>  
Reference: POLY 13990

To appear in: *Polyhedron*

Received Date: 9 April 2019  
Revised Date: 28 May 2019  
Accepted Date: 30 May 2019

Please cite this article as: V. Gugulothu, J. Ahemed, M. Subburu, B. Yadagiri, R. Mittal, C. Prabhakar, S. Pola, Evolution of Physical and Photocatalytic Properties of New Zn(II) and Ru(II) complexes, *Polyhedron* (2019), doi: <https://doi.org/10.1016/j.poly.2019.05.065>

This is a PDF file of an unedited manuscript that has been accepted for publication. As a service to our customers we are providing this early version of the manuscript. The manuscript will undergo copyediting, typesetting, and review of the resulting proof before it is published in its final form. Please note that during the production process errors may be discovered which could affect the content, and all legal disclaimers that apply to the journal pertain.



**Evolution of Physical and Photocatalytic Properties of New Zn(II) and Ru(II) complexes**

Venkanna Gugulothu,<sup>a</sup> Jakeer Ahemed,<sup>a</sup> Mahesh Subburu,<sup>a</sup> Bhongiri Yadagiri,<sup>a</sup> Ritu Mittal,<sup>b</sup> Chetti Prabhakar<sup>b</sup> and Someshwar Pola<sup>a\*</sup>

**Abstract**

Synthesis of Zn (II) and Ru (II) complexes were reported by using N<sub>4</sub>-macrocyclic Schiff base ligands under solvothermal conditions. The newly synthesized Zn (II) and Ru (II) complexes have been characterized by various physico-chemical techniques such as elemental analysis, molar conductance, HRMS, TGA, FESEM, UV-vis, FT-IR, <sup>1</sup>H-NMR, and cyclic voltammetry. By using molar conductance studies, the complexes are formulated as [Zn(TPTTP)]Cl<sub>2</sub> and [Ru(TPTTP)Cl<sub>2</sub>]. C-H bond activation of an sp<sup>3</sup> group of methylstyrenes (converted into cinnamaldehydes) and C-H bond activation of the sp<sup>2</sup> bond of polycyclic aromatic hydrocarbons through photooxidation was examined in the presence of Zn(II) and Ru(II) complexes. Reusable activity studies and photostability of catalyst are investigated by using UV-visible spectra. Based on the results, higher catalytic activity of [Ru(TPTTP)Cl<sub>2</sub>] complex than [Zn(TPTTP)]Cl<sub>2</sub> complex in both C-H bond activation and photooxidation of aromatic hydrocarbons has been reported.

**Keywords:** Ru(II) and Zn(II) Complexes, C-H bond activation, Methylstyrenes, Photooxidation, Polycyclic aromatic hydrocarbons

<sup>a</sup>Department of Chemistry, Osmania University, Hyderabad, India

<sup>b</sup>Department of Chemistry, National Institute of Technology, Kurukshetra, India.

\*Corresponding author: E-mail address: somesh.pola@gmail.com Tel: + 919959972288

**Introduction**

Tetradentate macrocyclic Schiff base ligands and their metal complexes are of very attention in coordination chemistry due to broad applications in several fields such as material chemistry [1] and medicinal chemistry [2]. These ligands and metal complexes are examined due to their essential properties, such as their capability to photooxidation [3], and applications as C-H bond activation for generation of new organic functional materials [4]. Piperazine itself is achiral, but the usage of the simply existing chiral piperazines as building blocks mains to chiral macrocycles. Hence, piperazine is an outstanding choice as a multipurpose building block for the synthesis of achiral or chiral macrocycles [5]. Due to the overall structural resemblance of piperazine and glucose, the macrocycle consisting of piperazine as a significant building block would be structurally mimic to the cyclodextrins

[6]. There is a need to design an efficient and green catalytic system, which would activate under milder reaction conditions for many technologically important processes [7]. Jacobsen's Mn(Salen) complex has appeared as a significant catalyst for the oxidation of alkenes in the pharmaceutical industry [8, 9]. Oxidation of natural products such as terpenes to oxygenated products is of attention; subsequently, these products are converted into natural products [10]. The allylic oxidation of  $\alpha$ -pinene forms several products in that one of the products is d-*l*-verbenone which is significant due to its utilization in the synthesis of Taxol [11,12]. The Cu(II) 2-Quinoxalinol Salen is also reported as a very efficient catalyst for allylic oxidations [13-16]. Whereas these studies are originated to be appropriate, still several restrictions like harsh reaction conditions, complex workup and/or purification process, the formation of destructive wastes, low efficient group easiness, and high costs remain.

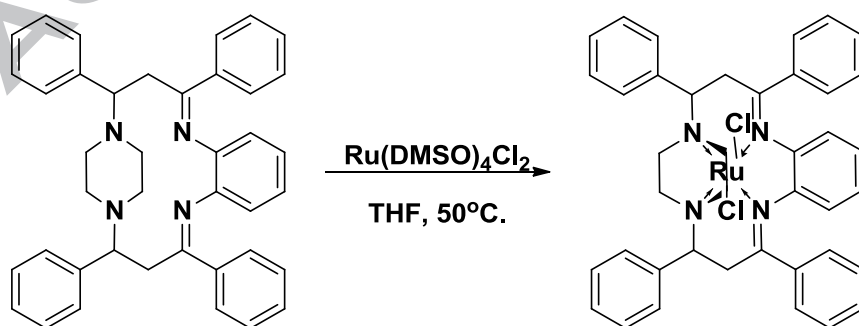
As part of our sustained attempts in the synthesis of metal complexes based on novel N, N and N, O donors as ligands and to investigate their applications in organic synthesis [17], studies have been led to exploring and know the photophysical, electrochemical and catalytic performance of macrocyclic ruthenium complexes [18-23]. These specific metal macrocyclic units can be utilized as preliminary building blocks to build the photo- and redox-active supramolecular systems. Therefore, complexes of different transition metal ions binding through macrocyclic ligands exhibited some significant properties such as a) the photophysical properties with bound metals, and b) the electrochemical communiqué between metal and ligand center. Lately, the amount of advancement in the chemistry of tetraazamacrocyclic ligands and their complexes in specific has been noticeable, since these structural motifs are engaging in various fields such as homogenous or heterogeneous catalysis [24-29]. In this connection, we report here the synthesis of new Zn(II), and Ru(II) macrocyclic Schiff's base complexes and their applications in C–H bond activation through  $sp^3$  and  $sp^2$  functional groups.

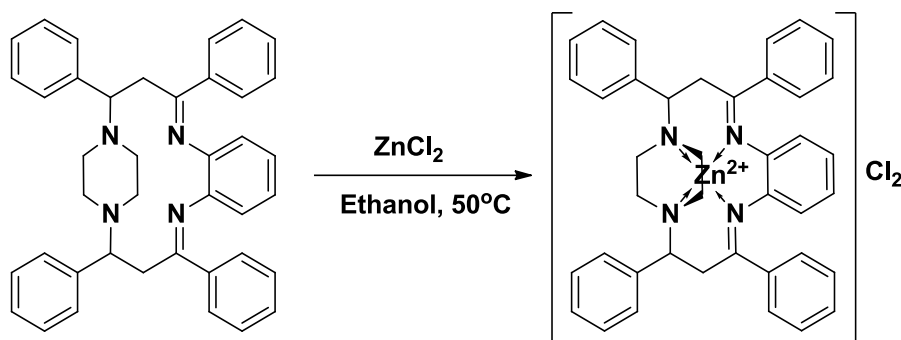
## 2. Experimental section and Characterization

### Materials and methods

All the starting materials procured from Sigma-Aldrich with the analytical grade. Solvents were distilled and dried by using standard techniques.  $[Ru(DMSO)_4Cl_2]$ , substituted methylstyrenes, methyl magnesium iodide, and other chemicals were purchased from TCI, India and all the solvents are analytical grade products from Merck. The purity of the compounds was monitored by TLC using Merck  $60F_{254}$  silica gel plates.

All the starting materials and solvents were directly used as obtained from the suppliers and recrystallized/redistilled as necessary. The SEM images captured on HITACHI SU-1500 variable pressure scanning electron microscope (VP-SEM). Thermograms of all samples were obtained using Shimadzu differential thermal analyzer (DTG-60H) with a heating rate of  $10^{\circ}\text{C min}^{-1}$  in the range from  $50^{\circ}\text{C}$  to  $1000^{\circ}\text{C}$  under Nitrogen purging rate of  $20\text{ mL/minute}$ . Brunauer-Emmett-Teller (BET) surface areas were determined by nitrogen adsorption-desorption isotherm measurements at  $77\text{ K}$  on a Quantachrome autosorb automated gas sorption system. CHN analyses were supported out utilizing Elemental Analyzer Flash EA 1112. Infrared spectra in KBr discs were recorded with a PerkinElmer BX series, Fourier Transforms infrared spectrophotometer.  $^1\text{H}$  and  $^{13}\text{C}$ - NMR spectra were recorded on a Bruker AV500 MHz Spectrometer. The HR FAB and HR documented mass spectra-EI methods on JMS-700 double focusing mass spectrometer with a high resolution of Mass Spectrometry Facility at ICT, Hyderabad, India. The conductance of the metal complexes was measured on Labline digital conductivity meter. Melting points were recorded on a Digital Melting Point Apparatus – 934 from Electronics India. The phases of the new materials were established by powder X-ray diffractometer (Miniflex, Rigaku) ( $\text{Cu K}\alpha$ ,  $\lambda=1.5406\text{ \AA}$  angle range of  $2\theta = 10^{\circ}$  to  $30^{\circ}$ ). The electronic spectra were measured in  $\text{C}_2\text{H}_4\text{Cl}_2/\text{CH}_3\text{CN}$  (1:1) solutions on LAMBDA 1050 UV/Vis Spectrophotometer. Cyclic voltammetry measurements were conducted on a PC-controlled CHI 62C electrochemical analyzer in a  $\text{C}_2\text{H}_4\text{Cl}_2$  solvent at a scan rate of  $100\text{ mVs}^{-1}$  using tetrabutylammonium perchlorate (0.1 M) as the supporting electrolyte. The glassy carbon, standard calomel electrode (SCE) and platinum wire were used as working, reference and counter electrodes, respectively. All the photoreactions were performed by using a multi-tube photo reactor system with LED visible light, Lelesil Innovative Systems, India. Preparation of M(II) complexes





**Scheme-1. Preparation of new Ru(II) and Zn(II) complexes**

*2.1. Preparation of the Ru(2,4,13,15-Tetraphenyl-1,5,12,16-tetraaza-tricyclo[14.2.2.0<sub>6,11</sub>]eicosa-4,6(11),7,9,12-pentaene)Cl<sub>2</sub>*

To 20 ml tetrahydrofuran (THF) solution of macrocyclic Schiff base ligand (2.00 mmol) corresponding Tetrakis(dimethylsulfoxide)dichlororuthenium(II) (2.00 mmol) was added with constant stirring at room temperature. Then the mixture was heated for five hours at 50°C. On cooling, the solid product was precipitated out and filtered, washed with cold THF and dried in a vacuum desiccator over fused CaCl<sub>2</sub>.

R<sub>f</sub> 0.22 (10% MeOH/CHCl<sub>3</sub>); elemental analysis expt. (calcd): C% 64.28 (64.34), H% 5.11 (5.13) N% 7.46 (7.50) Cl% 9.46 (9.50), and Ru% 13.34 (13.53); <sup>1</sup>H NMR (400MHz, *d*<sub>6</sub>-DMSO) δ (ppm) = 8.229 (m, 2H), 8.026 (m, 2H), 7.977 - 7.909 (m, 10H), 7.815 - 7.725 (m, 10H), 4.990 (m, 2H), 3.045 (s, 8H), 2.744 (d, 2H), and 2.324 (d, 2H); <sup>13</sup>C NMR (100 MHz *d*<sub>6</sub>-DMSO) δ (ppm) = 160.88, 143.24, 142.96, 137.50, 134.42, 128.57, 126.65, 124.79, 123.01, 122.07, 120.21, 120.12, 112.58, 108.40, 58.40, 34.21 and 20.22 MS (FAB): 747.19 (M+1)<sup>+</sup>; UV-Vis: 376.92, 402.48, and 418.24 nm.

*2.2. Preparation of the Zn(2,4,13,15-Tetraphenyl-1,5,12,16-tetraaza-tricyclo[14.2.2.0<sub>6,11</sub>]eicosa-4,6(11),7,9,12-pentaene)Cl<sub>2</sub>*

To 20 ml tetrahydrofuran (THF) solution of macrocyclic Schiff base ligand (2.00 mmol) corresponding ZnCl<sub>2</sub> (2.00 mmol) was added with constant stirring at room temperature. Then the mixture was refluxed for 5 h at 50°C. On cooling, the solid product was precipitated out and filtered, washed with cold THF and dried in a vacuum desiccator over fused CaCl<sub>2</sub>.

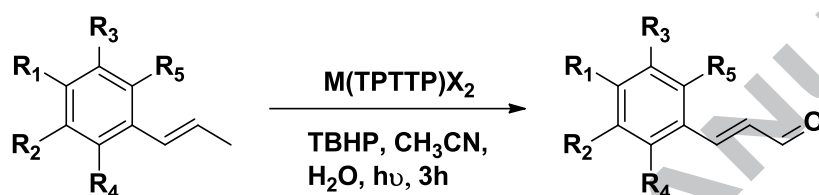
R<sub>f</sub> 0.28 (10% MeOH/CHCl<sub>3</sub>); elemental analysis expt. (calcd): C% 67.51 (67.57), H% 5.36 (5.39), N% 7.84 (7.88), Cl% 9.92 (9.97) and Zn% 8.99 (9.19); <sup>1</sup>H NMR (400MHz, *d*<sub>6</sub>-DMSO) δ (ppm) = 8.192 (m, 2H), 7.994 (m, 2H), 7.865 - 7.798 (m, 10H), 7.785 - 7.691 (m, 10H), 4.504 (m, 2H), 3.742 (s, 8H), 2.702 (d, 2H), and 2.318 (d, 2H); <sup>13</sup>C NMR (100 MHz

$d_6$ -DMSO)  $\delta$  (ppm) = 160.79, 143.52, 141.83, 138.83, 135.93, 133.48, 131.86, 128.77, 128.55, 126.51, 125.42, 125.12, 122.33, 118.72, 118.55, 111.47 57.41, 34.44 and 20.65 MS (FAB): 712.04 (M+1)<sup>+</sup>; UV-Vis: 362.13, 416.82, and 482.46 nm.

### 2.3. Catalytic activity studies

#### *C-H bond activation of methylstyrenes*

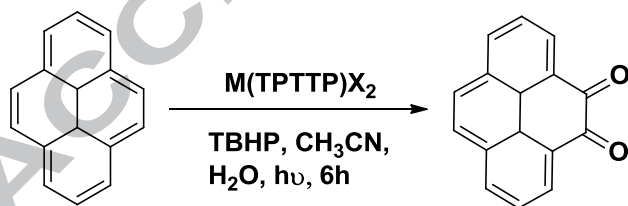
To a solution of Zn(II)/Ru(II) complex (1.25  $\mu$ mol), methylstyrenes (0.5 mmol) and TBHP (1.0 mmol) in 10 mL of acetonitrile was added at room temperature. After the reaction was stirred under visible light for three hours, (monitored the reaction by LC-MS) solvent was distilled under reduced pressure. Purification of crude products by column chromatography with hexane/dichloromethane (9:1, v/v) as eluent to an afforded pure product.



Scheme 2.

#### *General procedure for photooxidation*

To a solution of Zn(II)/ Ru(II) complex (1.25  $\mu$ mol), pyrene (0.5 mmol) and TBHP(1.0 mmol) in 10 mL of acetonitrile was added. After the reaction was stirred under visible light for 6 h, (monitored the reaction by LC-MS) solvent was evaporated using rotavapor. Purification of the crude compounds by column chromatography with dichloromethane/ethyl acetate (9:1, v/v) as eluent to an afforded pure product.



## 3. Result and Discussion

### 3.1. Molar conductivity measurements

The molar conductivities of the Zn(II) and Ru(II) complexes under investigation are measured for  $10^{-3}$ M solutions in various solvents such as DMF, DMSO, DMA, and NMP as presented in Table 1 and Table S1. For Ru (II) complexes have  $\Omega_M$  values in the range 8.0–12.0  $\text{ohm}^{-1} \text{cm}^2 \text{mol}^{-1}$  which indicate that the complex is non-electrolytes [30]. However, Zn(II)

complexes exhibited higher values in the range 121 – 124.2  $\text{ohm}^{-1}\text{cm}^2\text{mol}^{-1}$  which reveal that the complex is 1:2 electrolytic in nature [31]. The existence of chloride ions in Zn(II) complex is sensed by adding silver nitrate solution, immediately white precipitate was formed [32] and molar conductance was dropped.

**Table 1. Analytical and Physicochemical data of Zn(II) and Ru(II) complexes**

Compound	Calcd. Mol.w	Measured Mol. w m/z	% Yield	<sup>a</sup> M.P./D.P. (°C)	%C	%H	%N	%Cl	%M	$\Lambda_m \text{ ohm}^{-1} \text{ mol}^{-1} \text{ cm}^2$ (DMSO)
TPTTP C <sub>40</sub> H <sub>38</sub> N <sub>4</sub>	574.7	574.54	48	206	83.53 (83.59)	6.74 (6.66)	9.72 (9.75)	--	--	---
[Ru(TPTTP)Cl <sub>2</sub> ] C <sub>40</sub> H <sub>38</sub> Cl <sub>2</sub> N <sub>4</sub> Ru	746.73	747.19	51	312	64.28 (64.34)	5.11 (5.13)	7.46 (7.50)	9.46 (9.50)	13.34 (13.53)	8.34
[Zn(TPTTP)Cl <sub>2</sub> ] C <sub>40</sub> H <sub>38</sub> Cl <sub>2</sub> N <sub>4</sub> Zn	711.05	712.04	56	284	67.51 (67.57)	5.36 (5.39)	7.84 (7.88)	9.92 (9.97)	8.99 (9.19)	118.29

### 3.2 Thermal Analysis

All the metal complexes were pure and dried under vacuum at ambient conditions before studying their thermal stability. A weighed quantity of the complexes is heated at 200°C in the hot-air oven for 2 h. No weight loss or the change in the appearance of the complexes was observed. The thermal data is presented in Table 2, and typical thermograms are revealed in Figure 1. The single stage of decomposition occurs between 230 and 570 °C for both the complexes with a weight loss of 90.89 and 65.93 for [Zn(TPTTP)]Cl<sub>2</sub> and Ru(TPTTP)Cl<sub>2</sub> respectively, which matches to the loss of ligand molecule [32]. The weight of the final oxide left in the crucible was signifying the formation of respective metal oxide and the corresponding data shown in Table-2. The results of thermal analyses confirms the formulae of the complexes to be [M(L)] [where L = TPTTP and M = Zn(II) and Ru(II)] and conforms with the formula derived from elemental analyses data.

**Table –2: Thermal data of M(II) complexes**

Complex	Thermal Process	Temperature Range, °C	Pyrolysis product, %	
			Found	Calcd
[Zn(TPTTP)]Cl <sub>2</sub>	[Zn(TPTTP)]Cl <sub>2</sub> → [ZnO]	232.5 – 505.6	90.89	91.23
Ru(TPTTP)Cl <sub>2</sub>	[Ru(TPTTP)Cl <sub>2</sub> ] → [Ru <sub>2</sub> O <sub>3</sub> ]	306.8 – 562.5	65.93	66.50

### 3.3 FESEM analysis

The morphology of the complexes compared with ligand is completely changed in shape and size [33]. The SEM images of [Zn(TPTTP)]Cl<sub>2</sub> and Ru(TPTTP)Cl<sub>2</sub> complexes exposed that the particles are converted into like nanoplates type particles with variable shape and nano-octahedra as correlated with the ligand as shown in Figure 2. In this connection



surface area of the complexes are far higher than the ligands and values are presented in Table-3.

**Table 3. Surface area and Bandgap energies of ligands and Pd(II)-complexes**

Compound	Surface area (m <sup>2</sup> /g)	Bandgap energy (eV)		Onset value from UV spectra (nm)	
		Experimental Value	Theoretical Value	Experimental Value	Theoretical Value
TPTTP	14	3.48	4.08	356	382
[Ru(TPTTP)Cl <sub>2</sub> ]	68	2.23	2.39	556	518
[Zn(TPTTP)Cl <sub>2</sub> ]	32	2.84	3.51	436	353

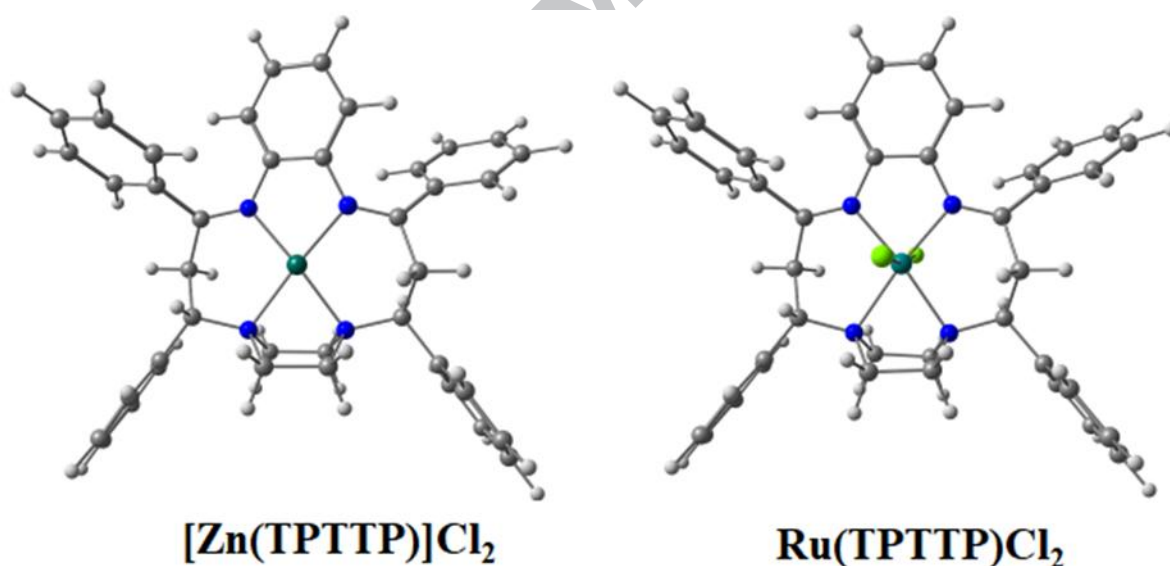
### 3.4 Spectral analysis of complexes

The mass spectra of the metal complexes were verified, and the data presented in Table 1. The mass spectra metal complexes were characterized by a peak corresponding to Schiff base fragmentation. The mass spectra of the complexes show some important peaks along with molecular ion peak (base peak) and these peaks matched with ligand mass and ligand fragments in the spectra (Figure 3). In the mass spectra of the complexes, the peaks at  $m/z$  712.04, and 747.74 can be represented to the molecular ion peaks ( $[ML]^{+1}$ ) ( $L = \text{TPTTP}$  and  $M = \text{Zn(II)}$  and  $\text{Ru(II)}$  complexes, respectively) [34, 35]. The fragmentation pathway of  $\text{Zn(TPTTP)Cl}_2$  complex as shown in Figure S1 and S2 and some of the significant peaks are identified which are matching with the spectral data. The IR spectra of the complexes were presented in Figure 4. There are some valuable peaks in the spectra of the complexes such as  $\nu(\text{C}=\text{N})$ ,  $\nu(\text{M}-\text{N})$  and  $\nu(\text{M}-\text{Cl})$ . The  $\nu(\text{C}=\text{N})$  stretching vibration is shown in the free ligand TPTTP at  $1628 \text{ cm}^{-1}$  [36]. This peak was shifted to lower wavenumber region by  $25 \text{ cm}^{-1}$  in both the complexes, signifying that the sharing of azomethine nitrogen in coordination to the metal ions. Similarly, the tertiary amine band also found to have shifted by  $40 \text{ cm}^{-1}$  confirming that the amine nitrogen atoms are involved in coordination [37]. New and most typical peaks found in the spectra of the metal complexes in the far-IR region and exhibited two important peaks at  $403$ , and  $436 \text{ cm}^{-1}$  are assignable to stretching vibrations of the  $\nu(\text{M}-\text{N})$  [38]. A band showed in the range of  $328 \text{ cm}^{-1}$  in the spectra of the Ruthenium complex designates as the existence of two chloride ions positioned trans to each other around metal center [38]. The IR spectral data confirm that TPTTP acts as neutral tetradentate ligand coordinating to the metal ions through azomethine-N, and tertiary amine-N atoms. This spectral data indicates that both the complexes ( $\text{Zn(II)}$  and  $\text{Ru(II)}$ ) are mononuclear.  $^1\text{H-NMR}$  spectra of  $\text{Zn(TPTTP)Cl}_2$  and  $\text{Ru(TPTTP)Cl}_2$  complexes recorded in  $d_6$ -DMSO. The resonance signals of azomethine [35]



and tertiary nitrogen atom attached methylene protons are shifted to the downfield side which indicating that the Zn(II) metal is coordination of TPTTP ligand. In the case of Ru(TPTTP)Cl<sub>2</sub> complex spectrum exhibited two significant changes compared with the ligand spectrum, i.e., imine and tertiary groups nitrogen atoms are coordination with Ru (II) ions. Then the Ar-Hs and tertiary –CH– protons are changed to the deshielding side as shown in Figure S3 and Figure 5. Similarly, all the peaks are shifted in <sup>13</sup>C-NMR spectra of both the complexes compared with ligand as shown in Figure 6 and 7.

The powder XRD outlines of the TPTTP ligand, [Ru(TPTTP)Cl<sub>2</sub>] and [Zn(TPTTP)]Cl<sub>2</sub> complexes showed 2θ peaks are presented in the range of 5 to 30 and high-intensity 2θ peaks at 16.5°, 10.2° and 9.3° respectively. However, [Ru(TPTTP)Cl<sub>2</sub>] and [Zn(TPTTP)]Cl<sub>2</sub> pattern were varied when compared with the pure ligand. Therefore, Ru<sup>2+</sup> and Zn<sup>2+</sup> ions have been coordinated with the N-atoms of the ligand. The powder XRD pattern for TPTTP ligand, [Ru(TPTTP)Cl<sub>2</sub>] and [Zn(TPTTP)]Cl<sub>2</sub> complexes are shown in figure S4. Therefore, complexes are very stable and coordinated with nitrogen atoms. Finally, based on spectroscopic data the Zn(II) and Ru(II) are coordinated as follows:



### *Electrochemical Properties*

The redox properties of [Zn(TPTTP)]Cl<sub>2</sub> and Ru(TPTTP)Cl<sub>2</sub> were examined using cyclic voltammetry in C<sub>2</sub>H<sub>4</sub>Cl<sub>2</sub>/CH<sub>3</sub>CN (1:1 ratio, 0.1 mol L<sup>-1</sup> n-Bu<sub>4</sub>NPF<sub>6</sub>). As shown in Figure 8, one-electron oxidation waves were noticed in the potential region -2.0 to + 2.0 V (vs Ag/AgCl). Estimation of their redox behaviors to that of TPTTP designates that the two oxidations around 0.695 V ( $E_{1/2}^1$ ) and 1.256 V ( $E_{1/2}^2$ ) are tertiary amine and imine based, which are derived from the sequential oxidation of neutral TPTTP to the radical cation (TPTTP<sup>•+</sup>) and then to the dication (TPTTP<sup>2+</sup>). Upon complexation ([Zn(TPTTP)]Cl<sub>2</sub>, and

[Ru(TPTTP)Cl<sub>2</sub>] complexes), the first oxidation potential is moved to the slightly more positive side [39-41], due to the electron-withdrawing inductive effect of the metal centric nature. However, the second oxidation potential also shifted towards negatively by 0.892 V. This shift can be explained by the electronic interactions between the TPTTP unit and the RuCl<sub>2</sub> produced by the shorter distance among them [42]. The third redox procedure at about  $E_{1/2}^3 = -1.452$  V can be designated to the Ru(II)-centered one-electron oxidation technique [43].

#### *Electronic spectra*

The electronic spectra of the complexes were measured in C<sub>2</sub>H<sub>4</sub>Cl<sub>2</sub>/CH<sub>3</sub>CN (1:1 ratio). The electronic spectra of the free ligand exhibited three bands at 321, 337 and 361 nm, indicates the  $\pi-\pi^*$  and  $n-\pi^*$  transitions in the aromatic ring and imine group [44]. The absorption spectra of complexes [Zn(TPTTP)]Cl<sub>2</sub> and Ru(TPTTP)Cl<sub>2</sub> in C<sub>2</sub>H<sub>4</sub>Cl<sub>2</sub>/CH<sub>3</sub>CN (1:1 ratio) at room temperature were recorded. As represented in Figure 9, intense absorption peaks are involving to the admixture of intraligand ( $\pi-\pi^*$ ) transitions of the TPTTP moiety and the Zn<sup>2+</sup> ions and are noticed in the range of 350–450 nm, which are red-shifted and more intense compared with the free ligand TPTTP. The redshift is sensible since the energy of the LUMO confined on the TPTTP is lowered upon coordination to Ru(II) [45]. In addition, complexes [Zn(TPTTP)]Cl<sub>2</sub> and Ru(TPTTP)Cl<sub>2</sub> also show broad bands at lower energy (350–600 nm), which could be indicated to the admixture of metal-to-ligand charge-transfer (MLCT,  $d\pi(\text{Ru}) \rightarrow \pi^*(\text{TPTTP})$ ) and ligand-to-ligand charge-transfer (LLCT) transitions [41,46].

#### *TDDFT Calculations*

The ground state geometry optimization of ligand (TPTTP), Zn(TPTTP)]Cl<sub>2</sub> and Ru(TPTTP)Cl<sub>2</sub> metal complexes are carried out in gas phase without any symmetric considerations by using DFT method at B3LYP level. The LANL2DZ effective core potential basis set was used for Zn and Ru metals [47], and 6-31G (d, p) basis set was used for ligand and H, C, N, and O-atoms of metal complexes. The calculated vibrational spectrum in all the optimized geometries has no imaginary frequencies, which indicates that all the optimized structures are located at the minimum point of the potential energy surface. Electronic absorption properties were carried out using the TDDFT methodologies at B3LYP functional for the optimized geometries. All the calculations were performed using the Gaussian09 software [48].

To get an understanding of absorption energies and optical band gap, we have supported out TDDFT calculations for these molecules. Calculated absorption energies for

ligand and metal complexes are shown in Table 4a and are well matched with the experiment. TPTTP shows maxima absorption at 382 nm with 0.019 oscillator strength, and meaningful contribution is between HOMO-1 to LUMO (51%) and HOMO to LUMO (45%). Zn (II) metal complex has an absorption maximum of 422 nm with 0.340 oscillator strength, and the main transition is between HOMO to LUMO (93%). In the case of Ru (II) complex, the first excited state is with low oscillator strength (0.001) showing absorption at 792 nm, and the transition is between HOMO to LUMO (92 %). The second excitation for Ru (II) complex is at 709 nm with 0.030 oscillator strength, and the major transition is from HOMO-1 to LUMO (92 %). Calculated absorption energies for ligand and metal complexes are shown in Table 4a and corresponding molecular orbital pictures are shown in Figure 10.

The calculated HOMO-LUMO gap (HLG) is dependable with the experimental band gap. It is evident from Table 4b. HOMO and LUMO levels of metal complexes are stabilized/destabilized when compared with its corresponding ligands, and the energy levels are shown graphically in Figure 11. The calculated HLG for TPTTP is 4.08 eV, and Zn(TPTTP)Cl<sub>2</sub> is 3.51 eV, it decreased the gap of 0.57 eV. Similarly, in the case of Ru(TPTTP)Cl<sub>2</sub> complex, the HLG is 2.39 eV, the difference in the gap concerning the ligand is of 1.69 eV. This decline in band gap from ligand to its metal complexes is due to the stabilization/destabilization of HOMO and LUMO levels of complexes, and corresponding values are shown in Table 4b.

**Table 4a. Absorption energies ( $\lambda$  in nm), Oscillator strength ( $f$ ), Transitions and Weight in % calculated at TD-B3LYP/6-31G (d, p) level of theory for B3LYP/6-31G (d, p) optimized geometries (for metals LANL2DZ basis set was used).**

Name	$\lambda^{\text{abs}}$	$f$	Transition	% Ci
TPTTP	382	0.019	H-1 -> L	51
			H -> L	45
[Zn(TPTTP)]Cl <sub>2</sub>	422	0.340	H -> L	93
[Ru(TPTTP)]Cl <sub>2</sub>	792	0.001	H-2 -> L	3
			H-1 -> L+1	2
			H -> L	92
	709	0.030	H-1 -> L	92

**Table 4b: Calculated energy levels of HOMO, LUMO and HOMO-LUMO Gap (HLG) are shown in eV.**

Compounds	TPTTP	[Zn(TPTTP)]Cl <sub>2</sub>	[Ru(TPTTP)]Cl <sub>2</sub>
→			
HOMO	-5.20	-11.34	-4.29
LUMO	-1.12	-7.83	-1.90

### 6. C-H bond activation of $sp^3$ -C of methylstyrenes (oxidation)

$\alpha$ ,  $\beta$ -Unsaturated aldehydes, mostly cinnamaldehydes, play a significant role in various fields such as food, pharmaceutical, and cosmetic industries [48–53] as well as substantial precursors for organic synthesis [54]. Hence, many applied approaches, including allylic alcohols oxidations [55], Peterson olefinations [56], formylation [57], Mannich reactions and cross-aldol condensations [58] and Saegusa oxidations [59,60] have been established for their preparation process. Still, these approaches are limited, comparatively harsh reaction setups, unapproachable reactants, high-cost catalysts, and/or unacceptable selectivity (Chemo- and regioselectivity). To overcome these disadvantages, a predominantly prominent another approach is C-H bond activation of  $sp^3$  carbon of methylstyrenes under visible light irradiation technique.

The Zn(II) and Ru(II) complexes of TPTTP were used as catalysts in the oxidation reactions to get cinnamaldehydes. The oxidation reactions were carried out on a millimole scale using 0.5 to 1.5 mol % catalyst charging. The oxidation reactions were examined in the presence and absence of various oxidizing agents such as  $H_2O_2$ /TBHP/*m*-CPBA with the catalyst in different solvents to optimize the conditions for better yields. In a typical reaction, the yield of the product, cinnamaldehyde, increased from 52% to 88% with TBHP as an oxidant in acetonitrile.

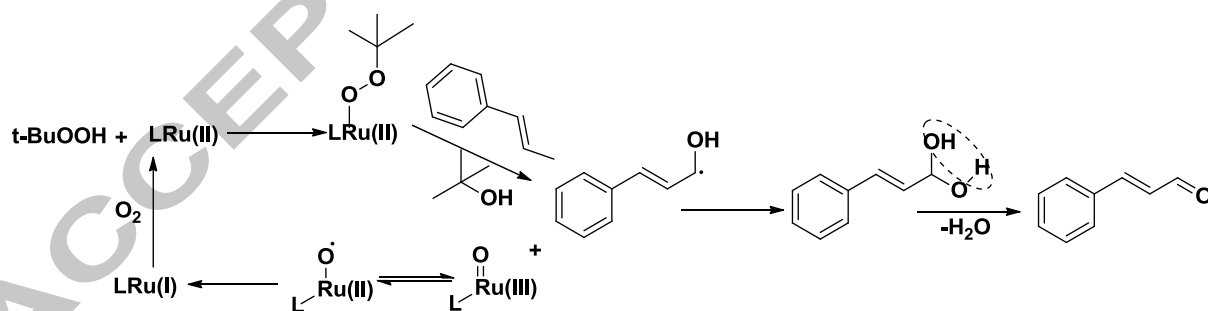
Further, a similar improvement in the yield was observed when TBHP was increased from 1 equiv. to 2 equiv. In other catalytic protocols reported [61], 10 to 12 equivalents of TBHP was used to complete the reaction. As anticipated, in the reaction mechanism only 2 equiv. of TBHP is essential for the oxidation of methylstyrenes to cinnamaldehydes. However, an excess of oxidant is used as some of the oxidants gets cinnamic acid as a byproduct. Therefore, evident from the investigations using  $H_2O_2$  which is known to decompose to a greater extent and required more than ten equivalents of  $H_2O_2$  in the oxidation reactions.

In the oxidation reactions using *m*-CPBA and  $[Zn(TPTTP)]Cl_2$  complex as a catalyst, it was observed that very less yield of products was formed and the mixture was too complex. Therefore, using two equiv. of TBHP and 1.25 mol % of the complex were used to study the influence of solvent systems on the oxidation of methylstyrene. Reactions progressed very slowly in  $CH_2Cl_2$ ,  $CHCl_3$ , DMSO, toluene, and DMF than  $CH_3CN$  as shown in figure 12. In this case, under inert conditions, only 26% yield was found in 3 h of reaction time as

compared to 92% yield in CH<sub>3</sub>CN solvent at normal atmospheric conditions. Therefore, which indicates that the contribution of O<sub>2</sub> in the oxidation of the various reactants in the presence of different complexes as catalysts.

C-H bond activation of a diversity of methylstyrenes was studied using 1.25 mol % of Zn(II) and Ru(II) complexes two equiv. of TBHP in CH<sub>3</sub>CN under visible light irradiation (Table 5). All of the reactants were transformed into the corresponding cinnamaldehydes in excellent yields within an average reaction time in the presence of Ru(TPTTP)Cl<sub>2</sub> when compared with the complexes of [Zn(TPTTP)]Cl<sub>2</sub> (Figure 13). The products were isolated and purified using flash column chromatography using hexane/dichloromethane (3:1) as eluent, resulting in a quite impressive isolated yield of 92% for liquid products, and the solid products were purified by recrystallization process.

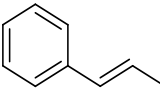
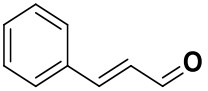
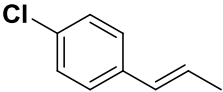
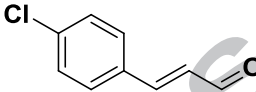
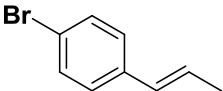

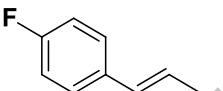
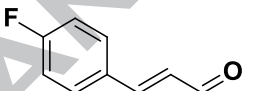
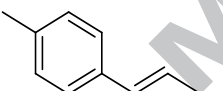
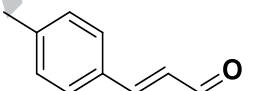
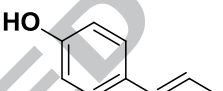
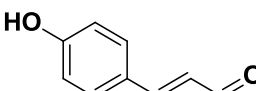
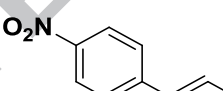
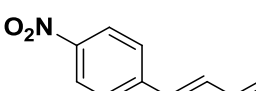
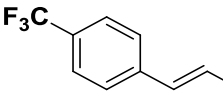
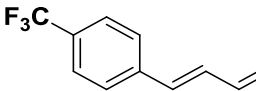
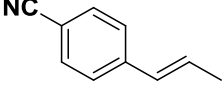
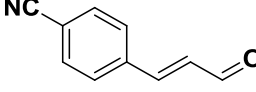
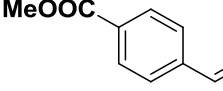
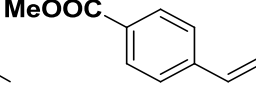
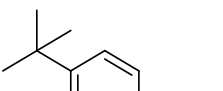
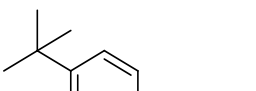
The C-H activation of methylstyrenes by the Ru(TPTTP)Cl<sub>2</sub> and [Zn(TPTTP)]Cl<sub>2</sub> complexes were performed as photocatalysts and based on results, Ru(TPTTP)Cl<sub>2</sub> exhibited more activity than [Zn(TPTTP)]Cl<sub>2</sub>. The optimized reaction conditions were used to carry out the oxidation reactions of methylstyrene by the Ru(TPTTP)Cl<sub>2</sub> and [Zn(TPTTP)]Cl<sub>2</sub> complexes as a catalyst, and the obtained data are given in Table 5. The Zn(II) complex showed low catalytic activity on all the substrates. The catalytic performance of the Ru(II) complex is similar or even improved than the activity demonstrated by some of the complexes reported earlier [62]. Ru(II) complex exhibited better catalytic activity than Zn(II) complex due to high surface area and low bandgap energy.

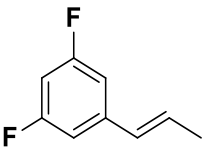
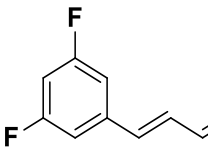
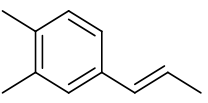
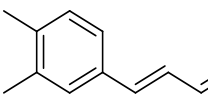
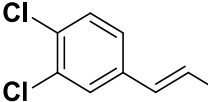
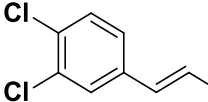
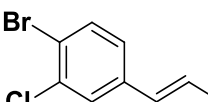
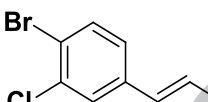


### Scheme 3 Proposed Catalytic Cycle for Oxidation Catalyzed by Ru(II) complex

The proposed mechanism of oxidation of allylic C-H group with TBHP involves binding of TBHP to the metal ion, homolytic cleavage of O-O bond followed by the formation of Ru(II)-oxo or Ru(III)-oxo bonds [63]. The plausible mechanism of oxidation reactions catalyzed by the Ru(II) complex is shown in scheme 3. Similarly, the plausible mechanism of oxidation reactions catalyzed by the Zn(II) complex through Zn(II)-oxo or Zn(I)-O<sup>•</sup> radicals and shown scheme S5 and another possible mechanism also possible and mentioned in scheme S6.

**Table 5. M(II) complexes of TPTTP Catalyzed C-H bond activation of  $sp^3$  - C of methylstyrenes (M = Zn and Ru) under visible light irradiation**

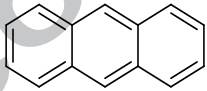
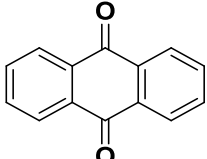
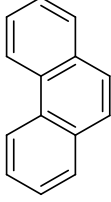
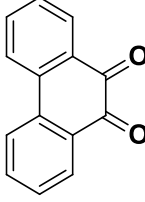
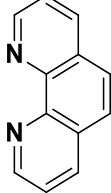
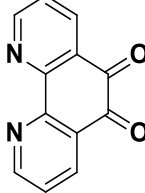
S. No.	Complex	Reactant	Product	Time (h)	% of Yield
1	[Zn(TPTTP)]Cl <sub>2</sub>			3	38
	Ru(TPTTP)Cl <sub>2</sub>			3	92
2	[Zn(TPTTP)]Cl <sub>2</sub>			3	36
	Ru(TPTTP)Cl <sub>2</sub>			3	85
3	[Zn(TPTTP)]Cl <sub>2</sub>			3	29
	Ru(TPTTP)Cl <sub>2</sub>			3	78
4	[Zn(TPTTP)]Cl <sub>2</sub>			3	31
	Ru(TPTTP)Cl <sub>2</sub>			3	76
5	[Zn(TPTTP)]Cl <sub>2</sub>			3	35
	Ru(TPTTP)Cl <sub>2</sub>			3	81
6	[Zn(TPTTP)]Cl <sub>2</sub>			3	37
	Ru(TPTTP)Cl <sub>2</sub>			3	83
7	[Zn(TPTTP)]Cl <sub>2</sub>			3	31
	Ru(TPTTP)Cl <sub>2</sub>			3	76
8	[Zn(TPTTP)]Cl <sub>2</sub>			3	27
	Ru(TPTTP)Cl <sub>2</sub>			3	79
9	[Zn(TPTTP)]Cl <sub>2</sub>			3	24
	Ru(TPTTP)Cl <sub>2</sub>			3	73
10	[Zn(TPTTP)]Cl <sub>2</sub>			3	33
	Ru(TPTTP)Cl <sub>2</sub>			3	74
11	[Zn(TPTTP)]Cl <sub>2</sub>			3	21
	Ru(TPTTP)Cl <sub>2</sub>			3	69

12	[Zn(TPTTP)]Cl <sub>2</sub>			3	26
	Ru(TPTTP)Cl <sub>2</sub>			3	81
13	[Zn(TPTTP)]Cl <sub>2</sub>			3	23
	Ru(TPTTP)Cl <sub>2</sub>			3	78
14	[Zn(TPTTP)]Cl <sub>2</sub>			3	21
	Ru(TPTTP)Cl <sub>2</sub>			3	73
15	[Zn(TPTTP)]Cl <sub>2</sub>			3	36
	Ru(TPTTP)Cl <sub>2</sub>			3	85

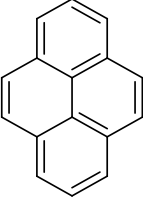
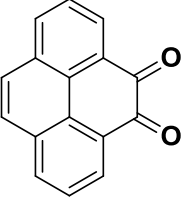
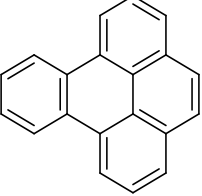
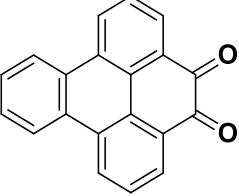
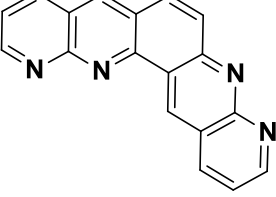
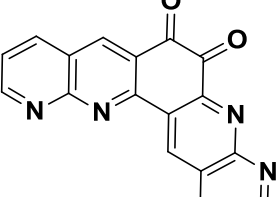
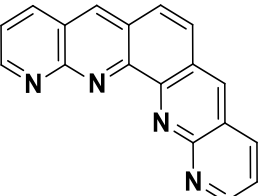
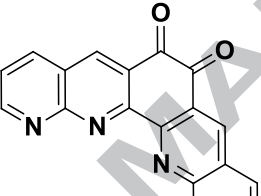
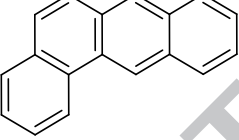
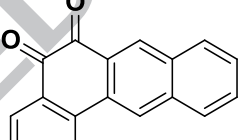
### Sp<sup>2</sup> C-H bond activation

Oxidation of polycyclic aromatic hydrocarbons (PAHs) is one of a very significant process for generating new heterocyclic fused PAHs [64-71]. Oxidation of PAHs with reported protocols was meager yield, and various byproducts are formed, and the purification process is very tough for required compounds. For this reason, using new Ru(TPTTP)Cl<sub>2</sub> complex acts as a photocatalyst for photooxidation of PAHs under visible light irradiation technique. Based on the above allylic oxidation of methylstyrenes, photooxidation of PAHs also examined under the same conditions for the formation of diones and presented in Table 6.

**Table 6. Photooxidation of PAHs in the presence of Ru(TPTTP)Cl<sub>2</sub> under visible light irradiation**

S.No.	Reactant	Product	Complex	Time (h)	% of Yield
1			[Ru(TPTTP)Cl <sub>2</sub> ] [Zn(TPTTP)]Cl <sub>2</sub>	6	74 36
2			[Ru(TPTTP)Cl <sub>2</sub> ] [Zn(TPTTP)]Cl <sub>2</sub>	6	78 32
3			[Ru(TPTTP)Cl <sub>2</sub> ] [Zn(TPTTP)]Cl <sub>2</sub>	6	73 27



4			[Ru(TPTTP)Cl <sub>2</sub> ] [Zn(TPTTP)]Cl <sub>2</sub>	6 41	85 41
5			[Ru(TPTTP)Cl <sub>2</sub> ] [Zn(TPTTP)]Cl <sub>2</sub>	6 39	80 39
6			[Ru(TPTTP)Cl <sub>2</sub> ] [Zn(TPTTP)]Cl <sub>2</sub>	6 33	78 33
7			[Ru(TPTTP)Cl <sub>2</sub> ] [Zn(TPTTP)]Cl <sub>2</sub>	6 28	73 28
8			[Ru(TPTTP)Cl <sub>2</sub> ] [Zn(TPTTP)]Cl <sub>2</sub>	6 21	65 21

Optimization of reaction conditions with pyrene and tetraphene in the presence of various catalysts commercial and present catalysts such as [Zn(TPTTP)]Cl<sub>2</sub>, and Ru(TPTTP)Cl<sub>2</sub> (5% mol) under visible light irradiation and shown in figure 14.

### Conclusion

In this work, we summarized the synthesis and characterization of new two Schiff base macrocyclic ligand based complexes with Zn(II) and Ru(II). The newly synthesized metal complexes are investigated by analytical, thermal, spectroscopic and electrochemical studies. We studied sp<sup>3</sup> and sp<sup>2</sup> C-H bond activation via photooxidation conditions using [Zn(TPTTP)]Cl<sub>2</sub> and Ru(TPTTP)Cl<sub>2</sub> complexes for methylstyrenes and polycyclic aromatic hydrocarbons different substrates and solvent effect. The Ru(II) complex exhibited excellent catalytic activity in the oxidation of all the substrates to convert the desired oxidized products.

### Supporting Information

Spectral data of complexes and  $\alpha$ ,  $\beta$ -unsaturated aldehydes such as  $^1\text{H-NMR}$ , and Mass spectra included in are inserted supporting information part (Figure S7 - S47).

#### ACKNOWLEDGMENT

SP and CP thanks to SERB - New Delhi, India for financial support under UGC-MRP 6417/16 (SERO/UGC) and SB/FT/CS-101/2014 respectively and thanks to DST-FIST, New Delhi. CP thank CSIR, New Delhi, India for financial support under EMR-II grant (No. 02(0339)/18/EMR-II). Special thankful to Prof. Yu-Tai Tao, Institute of Chemistry, Academia Sinica, Taipei, Taiwan, for providing FESEM data.

#### References

- [1] V. C. Gibson, C. Redshaw, G. A. Solan, *Chem. Rev.*, 107 (2007) 1745–1776.
- [2] M. Białek, A. Białońska, L. Latos-Grażyński, *Inorg. Chem.*, 54 (2015) 6184–6194.
- [3] D. E. De Vos, B. F. Sels, P. A. Jacobs, *Adv. Synth. Catal.* 345 (2003) 457-473.
- [4] S. Lee, E. A. Kapustin, O. M. Yaghi, *Science*, 353 (2016) 808–811.
- [5] H. Keypour, M. Rezaeivala, L. Valencia, P. P.-Lourido, A. H. Mahmoudkhani, *Polyhedron* 28 (2009) 3415–3418.
- [6] X.-J. Jiang, M. Li, H.-L. Lu, L.-H. Xu, H. Xu, S.-Q. Zang, M.-S. Tang, H.-W. Hou, T. C. W. Mak, *Inorg. Chem.*, 53 (2014) 12665–12667.
- [7] K. Rissanen, J. Huuskonen, A. Koskinen, *J. Chem. Soc., Chem. Commun.* (1993) 771-772.
- [8] T. Katsuki, *Coord. Chem. Rev.* 140 (1995) 189-214
- [9] W. Zhang, J. L. Loebach, S. R. Wilson, E. N. Jacobson, *J. Am. Chem. Soc.* 112 (1990) 2801- 2803.
- [10] G. Rothenberg, Y. Yatziv, Y. Sasson, *Tetrahedron*, 54 (1998) 593 – 598.
- [11] P.A. Wende, T.P. Muciaro, *J. Am. Chem. Soc.* 114 (1992) 5878- 5879.
- [12] M.R. Sivik, K.J. Santon, L.A. Paquette, *Org. Synth.* 72 (1994) 57.
- [13] Y. Li, T. B. Lee, T. Wang, A. V. Gamble, A. E. V. Gorden, *J. Org. Chem.*, 77 (2012) 4628–4633.
- [14] K. C. Weerasiri, A. E. V. Gorden, *Tetrahedron*, 70 (2014) 7962-7968.
- [15] Y. Li, T. B. Lee, K. Weerasiri, T. Wang, E. E. Buss, M. L. McKee A. E. V. Gorden, *Dalton Trans.*, 43 (2014) 13578-13583.
- [16] X. Wu, A. E. V. Gorden, (2009) 503-509.
- [17] T. Katsuki, *J. Mol. Catal. A Chem.*, 113 (1996) 87-107.

- [18] E. C. Constable, C. E. Housecroft, M. Neuburger, P. J. Rösel, S. Schaffner, J. A. Zampese, *Chem. -Eur. J.*, 2009, 15, 11746-11757.
- [19] O. Henze, D. Lentz, A. Schäfer, P. Franke, A. D. Schlüter, *Chem. -Eur. J.*, 2002, 8, 357-365.
- [20] C. Kaes, M. Wais Hosseini, C. Kaes, A. De Cian, J. Fischer, *Chem. Commun.*, 1997, 2229-2230.
- [21] P. D. Beer, F. Szemes, V. Balzani, C. M. Salà, M. G. B. Drew, S. W. Dent, M. Maestri, *J. Am. Chem. Soc.*, 1997, 119, 11864-11875.
- [22] M. Venturi, F. Marchioni, B. Ferrer Ribera, V. Balzani, D. M. Opris, A. D. Schlüter, *ChemPhysChem*, 2006, 7, 229-239.
- [23] M. Venturi, F. Marchioni, V. Balzani, Dorina M. Opris, O. Henze, A. D. Schlüter, *Eur. J. Org. Chem.*, 2003, 2003, 4227-4233.
- [24] S. Zolezzi, E. Spodine, A. Decinti, *Polyhedron* 21 (2002) 55–59.
- [25] C.D. Sulok, J.L. Bauer, A.L. Speelman, B. Weber, N. Lehnert, *Inorg. Chim. Acta*, 380 (2012) 148–160.
- [26] L.K. Gupta, S. Chandra, *Transit. Metal Chem.*, 31 (2006) 368–373.
- [27] P.M. Reddy, A.V.S.S. Prasad, V. Ravinder, *Transit. Metal Chem.*, 32 (2007) 507–513.
- [28] K. Shanker, P.M. Reddy, R. Rohini, Y.P. Ho, V. Ravinder, *J. Coord. Chem.*, 62 (2009) 3040–3049.
- [29] B. Geeta, K. Shrivankumar, P.M. Reddy, E. R. Krishna, M. Sarangapani, K.K. Reddy, V. Ravinder, *Spectrochim. Acta A*, 77 (2010) 911–915.
- [30] E. R. Krishna, P. M. Reddy, M. Sarangapani, G. Hanmanthu, B. Geeta, K. S. Rani, V. Ravinder, *Spectrochim. Acta A*, 97 (2012) 189–196.
- [31] M. Sivagamasundari, R. Ramesh, *Spectrochimica Acta Part A*, 67 (2007) 256-262.
- [32] K. Shanker, P.M. Reddy, R. Rohini, Y.P. Ho, V. Ravinder, *J. Coord. Chem.*, 62 (2009) 3040–3049.
- [33] S. Pola, Y. Bhongiri, R. Jadhav, P. Chetti, G. Venkanna, *RSC Adv.*, 6 (2016) 88321–88331.
- [34] N. Shan, S. M. Hawxwell, H. Adams, L. Brammer, J. A. Thomas, *Inorg. Chem.*, 47 (2008) 11551-11560.
- [35] S. J. Swamy, S. Pola, *Spectrochim. Acta A*, 70 (2008) 929–933.
- [36] P.M. Reddy, A.V.S.S. Prasad, Ch. K. Reddy, V. Ravinder, *Transit. Metal Chem.* 33 (2008) 251–258.

- [37] A. Prasad, P.M. Reddy, K. Shanker, R. Rohini, V. Ravinder, *Color. Technol.* 125 (2009) 284–287.
- [38] A.K. Mohamed, K.S. Islam, S.S. Hasan, M. Shakir, *Transit. Metal Chem.* 24 (1999) 198–201.
- [39] A. Juris, V. Balzani, F. Barigelletti, S. Campagna, P. Belser, A. von Zelewsky, *Coord. Chem. Rev.*, 84 (1988) 85-277.
- [40] J. Qin, S. Y. Deng, C. X. Qian, T. Y. Li, H. X. Ju, J. L. Zuo, *J. Organomet. Chem.*, 750 (2014) 7–12.
- [41] J. Qin, L. Hu, N. Lei, Y.-F. Liu, K.-K. Zhang, J.-L. Zuo, *Acta Chim. Slov.*, 61 (2014) 740–745.
- [42] L. Hu, W. Liu, C. H. Li, X. H. Zhou, J. L. Zuo, *Eur. J. Inorg. Chem.*, 35 (2013) 6037–6048.
- [43] L. K. Keniley, L. J. Ray, K. Kovnir, L. A. Dellinger, J. M. Hoyt, M. Shatruk, *Inorg. Chem.* 49 (2010) 1307–1309.
- [44] C. Goze, N. Dupont, E. Beitler, C. Leiggenger, H. Jia, P. Monbaron, S. X. Liu, A. Neels, A. Hauser, S. Decurtins, *Inorg. Chem.*, 47 (2008) 11010–11017.
- [45] J. Qin, L. Hu, G. N. Li, X. S. Wang, Y. Xu, J. L. Zuo, X. Z. You, *Organometallics*, 30 (2011) 2173–2179.
- [46] R. Zong, F. Naud, C. Segal, J. Burke, F. Wu, R. Thummel, *Inorg. Chem.* 2004, 43, 6195–6202.
- [47] P.J. Hay, W.R. Wadt, *J. Chem. Phys.* 82 (1985) 270.
- [48] M. J. Frisch, G. W. Trucks, H. B. Schlegel, G. E. Scuseria, M. A. Robb, J. R. Cheeseman, G. Scalmani, V. Barone, B. Mennucci, G. A. Petersson, H. Nakatsuji, M. Caricato, X. Li, H. P. Hratchian, A. F. Izmaylov, J. Bloino, G. Zheng, J. L. Sonnenberg, M. Hada, M. Ehara, K. Toyota, R. Fukuda, J. Hasegawa, M. Ishida, T. Nakajima, Y. Honda, O. Kitao, H. Nakai, T. Vreven, J. A. Montgomery, Jr., J. E. Peralta, F. Ogliaro, M. Bearpark, J. J. Heyd, E. Brothers, K. N. Kudin, V. N. Staroverov, R. Kobayashi, J. Normand, K. Raghavachari, A. Rendell, J. C. Burant, S. S. Iyengar, J. Tomasi, M. Cossi, N. Rega, J. M. Millam, M. Klene, J. E. Knox, J. B. Cross, V. Bakken, C. Adamo, J. Jaramillo, R. Gomperts, R. E. Stratmann, O. Yazyev, A. J. Austin, R. Cammi, C. Pomelli, J. W. Ochterski, R. L. Martin, K. Morokuma, V. G. Zakrzewski, G. A. Voth, P. Salvador, J. J. Dannenberg, S. Dapprich, A. D. Daniels, O. Farkas, J. B. Foresman, J. V. Ortiz, J. Cioslowski, and D. J. Fox, *Gaussian 09, Revision A.02*, Gaussian, Inc., Wallingford CT, 2009.
- [49] J. M. Fang, S. A. Chen, Y. S. Cheng, *J. Agric. Food Chem.*, 37 (1989) 744-746.

- [50] G. Singh, S. Maurya, M. P. de Lampasona, C. A. N. Catalan, *Food Chem. Toxicol.*, 45 (2007) 1650 -1661.
- [51] H. Ferhout, J. Bohatier, J. Guillot, J. C. Chalchat, *J. Essent. Oil Res.*, 11 (1999) 119-129.
- [52] M. Friedman, P. R. Henika, R. E. Mandrell, *J. Food Protect.*, 65 (2002) 1545-1560.
- [53] S.-T. Chang, S.-S. Cheng, *J. Agric. Food Chem.*, 50 (2002) 1389- 1392.
- [54] E. F. Glorius, in *Science of Synthesis*, ed. R. Bruckner, Georg Thieme Verlag, Stuttgart, 25 (2007) 733.
- [55] M. Reid, D. J. Roweb, R. J. Taylor, *Chem. Commun.*, (2003) 2284-2285.
- [56] D. J. Ager, *Synthesis*, (1984) 384.
- [57] H. Neumann, A. Sergeev, M. Beller, *Angew. Chem., Int. Ed.*, 47 (2008) 4887-.
- [58] (a) P. R. Mackie and C. E. Foster, in *Comprehensive Organic Group Transformations II*, ed. A. R. Katritzky, R. J. K. Taylor, K. Jones, Elsevier, Dordrecht, 3 (2004) 59–97.
- [59] S. Porth, J. W. Bats, D. Trauner, G. Giester, J. Mulzer, *Angew. Chem., Int. Ed.*, 38 (1999) 2015-.
- [60] Y. Li, T. B. Lee, T. Wang, A. V. Gamble, A. E. V. Gordon *J. Org. Chem.*, 77 (2012) 4628–4633.
- [61] T. Storr, P. Verma, R.C. Pratt, E.C. Wasinger, Y. Shimazaki, T.D.P. Stack, *J. Am. Chem. Soc.* 130 (2008) 15448- .
- [62] L. K. Stultz, M. H. V. Huynh, R. A. Binstead, M. Curry, T. J. Meyer, *J. Am. Chem. Soc.*, 122 (2000) 5984–5996.
- [63] T. T. Ponduru, C. Qiu, J. X. Mao, A. Leghissa, J. Smuts, K. A. Schug, H. V. R. Dias, *New J. Chem.*, 2018,42, 19442-19449.
- [64] L.T.-Murciano, A. Gilbank, B. Puertolas, T. Garcia, B. Solsona, D. Chadwick, *Appl. Catal. B: Environ.*, 132–133 (2013) 116-122.
- [65] A. C. Estrada, M. M. Q. Simões, I. C. M. S. Santos, M. G. P. M. S. Neves, J. A. S. Cavaleiro, A. M. V. Cavaleiro, 3 (2011) 771-779.
- [66] N. G. G. Shive, M. S. Chauhan, *Catal. Commun.*, 10 (2009) 383-387.
- [67] A. Sorokin, B. Meunier, (1998) 1269-1281.
- [68] A. Gold, K. Jayaraj, L. M. Ball, K. Brust, *J. Mol. Catal. A: Chem.*, 125 (1997) 23-32.
- [69] J. S. Ewsi, *Tetrahedron*, 40 (1984) 4997-5000.
- [70] J. Kou, Z. Li, Y. Yuan, H. Zhang, Y. Wang, Z. Zou, *Environ. Sci. Technol.*, 43 (2009) 2919–2924.
- [71] J. Hu, D. Zhang, F. W. Harris, *J. Org. Chem.*, 70 (2005) 707–708.

**Fig. 1** Thermograms images for a)  $[\text{Zn}(\text{TPTTP})]\text{Cl}_2$  and b)  $\text{Ru}(\text{TPTTP})\text{Cl}_2$  of complexes.

**Fig. 2** FESEM images of a) ligand TPTTP; b)  $[\text{Zn}(\text{TPTTP})]\text{Cl}_2$  and c)  $\text{Ru}(\text{TPTTP})\text{Cl}_2$  of complexes.

**Fig. 3**  $[\text{Zn}(\text{TPTTP})]\text{Cl}_2$  of mass spectral fragmentation pathway.

**Fig. 4** IR spectral pattern of  $[\text{Zn}(\text{TPTTP})]\text{Cl}_2$  and  $\text{Ru}(\text{TPTTP})\text{Cl}_2$  of complexes.

**Fig. 5**  $^1\text{H}$ -NMR spectra of ligand and  $\text{Ru}(\text{TPTTP})\text{Cl}_2$

**Fig. 6**  $^{13}\text{C}$ -NMR Spectra of  $[\text{Ru}(\text{TPTTP})\text{Cl}_2]$

**Fig. 7**  $^{13}\text{C}$ -NMR spectra of ligand and  $[\text{Zn}(\text{TPTTP})]\text{Cl}_2$

**Fig. 8** Cyclic voltammograms for a) ligand, b)  $[\text{Zn}(\text{TPTTP})]\text{Cl}_2$  and c)  $\text{Ru}(\text{TPTTP})\text{Cl}_2$  of complexes.

**Fig. 9** Electronic spectra of a) ligand; b)  $[\text{Zn}(\text{TPTTP})]\text{Cl}_2$  and c)  $\text{Ru}(\text{TPTTP})\text{Cl}_2$  of complexes.

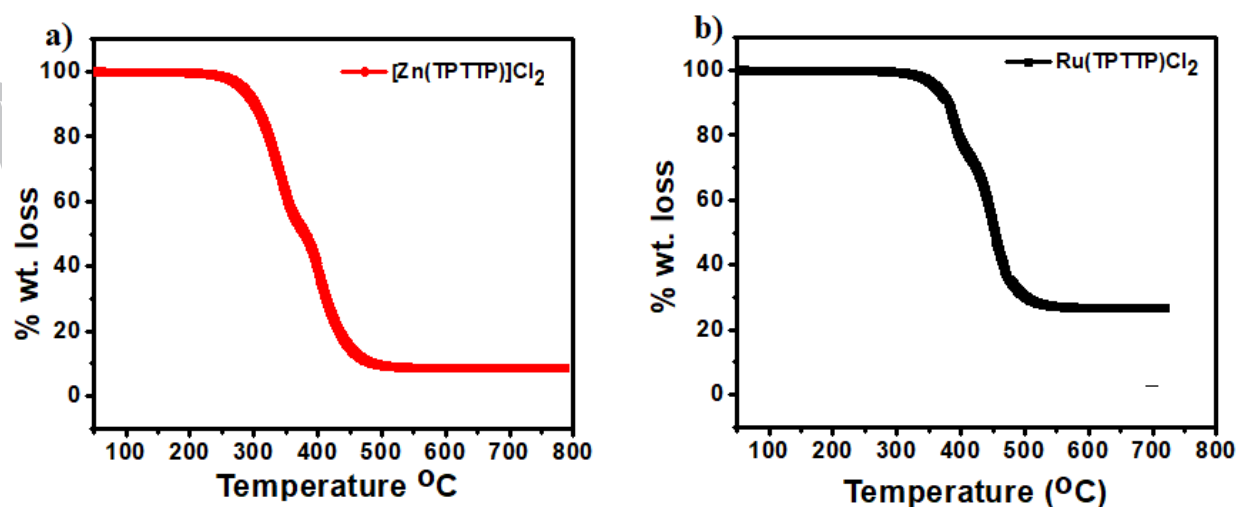
**Fig. 10** HOMO-LUMO images of TPTTP,  $[\text{Zn}(\text{TPTTP})]\text{Cl}_2$  and  $\text{Ru}(\text{TPTTP})\text{Cl}_2$ .

**Fig. 11** Graphical representation of HOMO-LUMO bandgap energies of TPTTP,  $\text{Zn}(\text{TPTTP})\text{Cl}_2$  and  $\text{Ru}(\text{TPTTP})\text{Cl}_2$

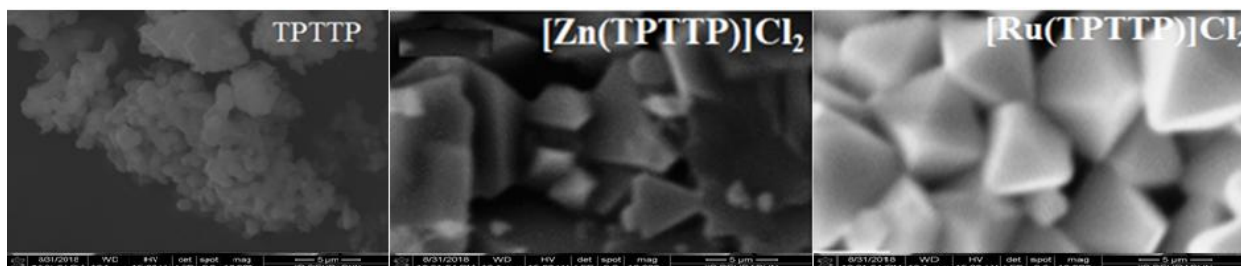
**Fig. 12** Effect of solvent and their rate of conversion under visible light irradiation.

**Fig. 13** Effect of complex on rate of conversion each reactant under visible light irradiation.

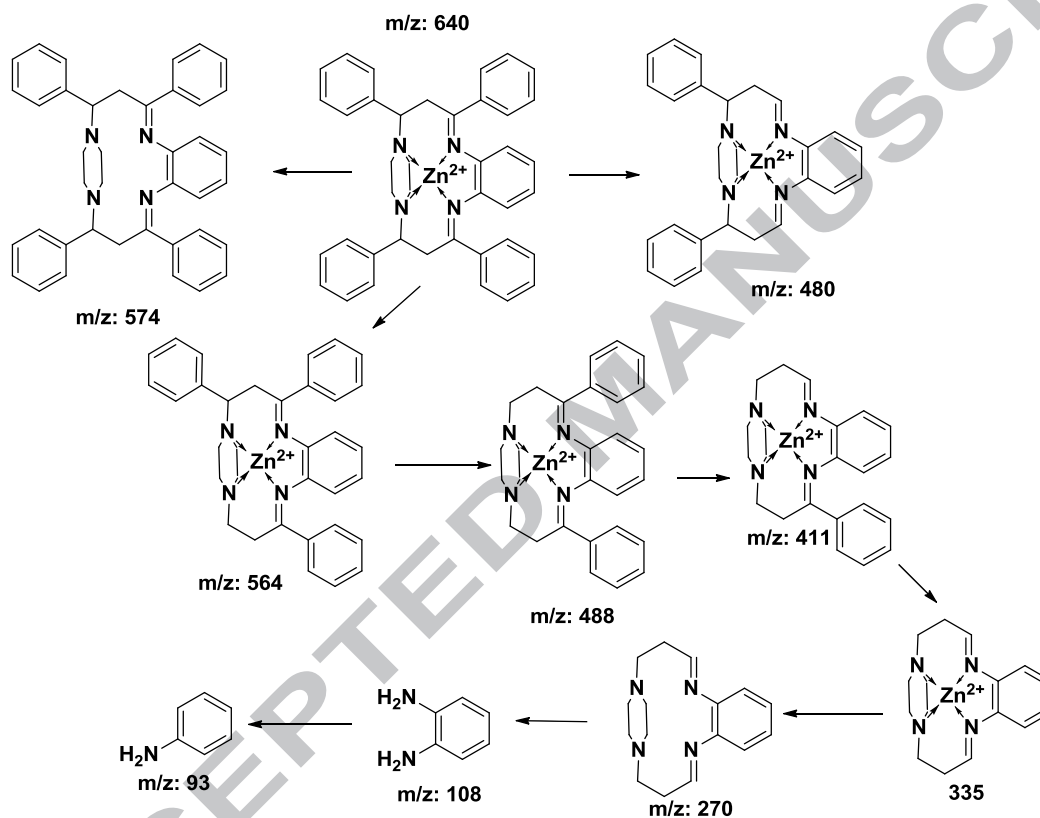
**Fig. 14** Optimization reaction conditions in the presence of various catalytic system under visible light irradiation.



**Fig. 1** Thermograms images for a)  $[\text{Zn}(\text{TPTTP})]\text{Cl}_2$  and b)  $\text{Ru}(\text{TPTTP})\text{Cl}_2$  of complexes.



**Fig. 2** FESEM images of a) ligand TPTTP; b)  $[\text{Zn}(\text{TPTTP})]\text{Cl}_2$  and c)  $[\text{Ru}(\text{TPTTP})]\text{Cl}_2$  of complexes.



**Fig. 3**  $[\text{Zn}(\text{TPTTP})]\text{Cl}_2$  of mass spectral fragmentation pathway.



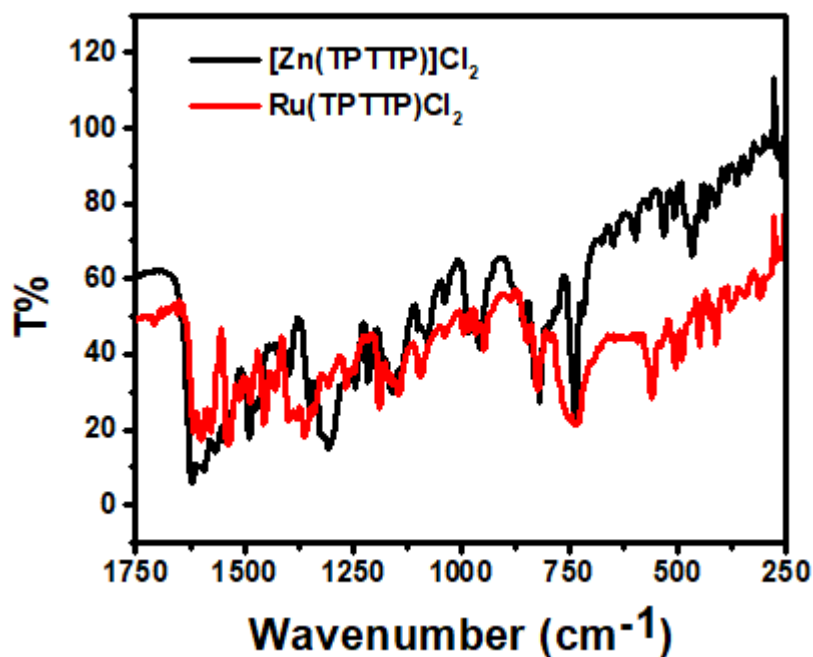


Fig. 4 IR spectral pattern of  $[\text{Zn}(\text{TPTTP})]\text{Cl}_2$  and  $\text{Ru}(\text{TPTTP})\text{Cl}_2$  of complexes.

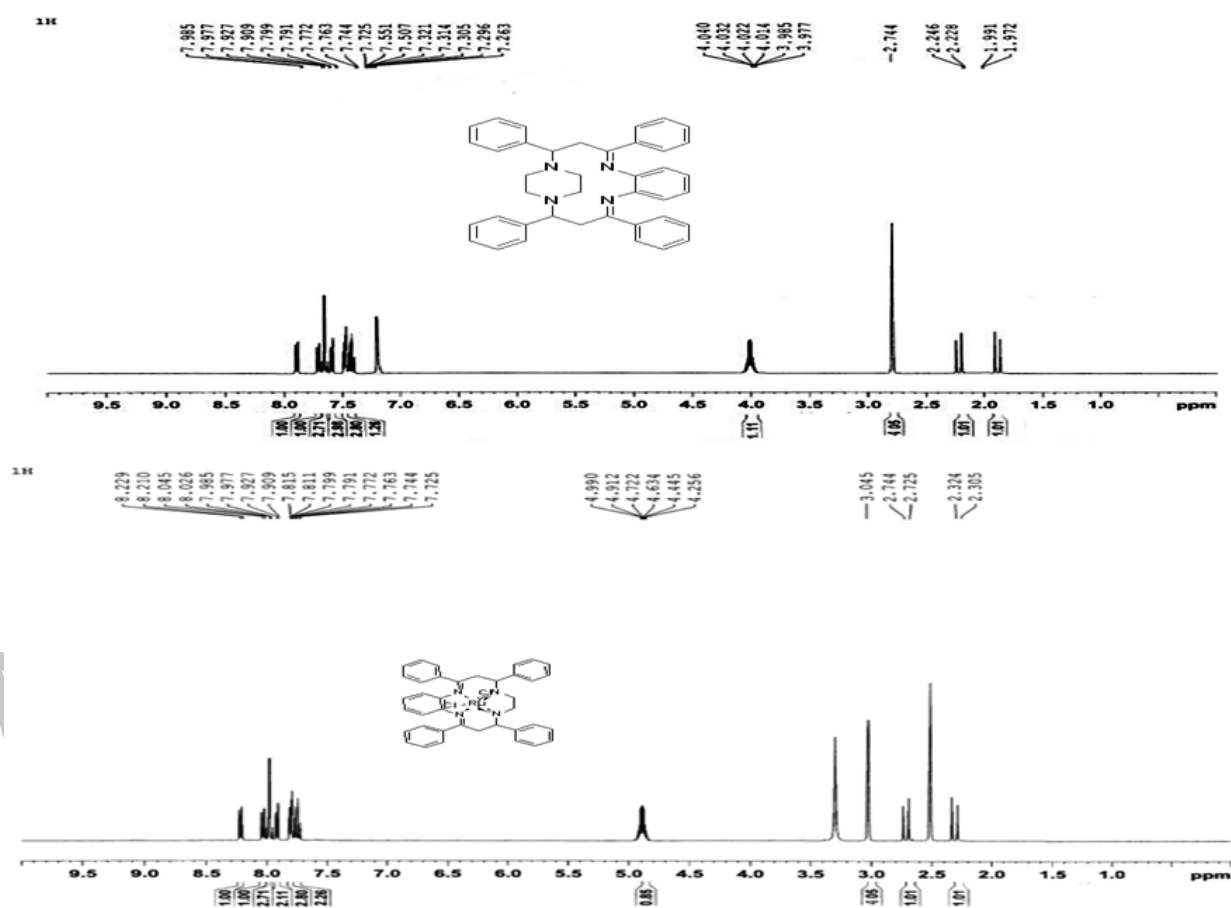


Fig. 5  $^1\text{H-NMR}$  spectra of ligand and  $\text{Ru}(\text{TPTTP})\text{Cl}_2$

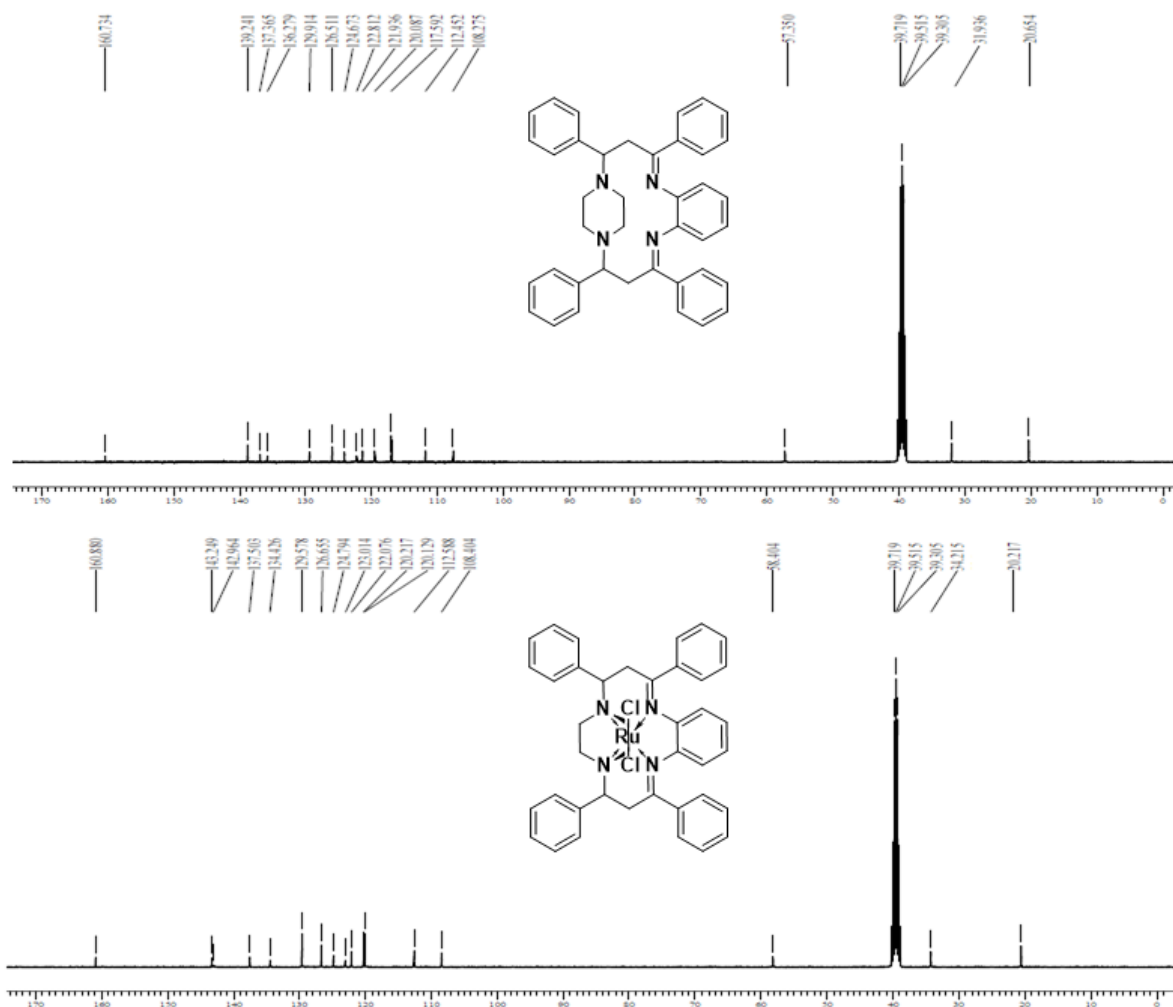


Fig. 6  $^{13}\text{C}$ -NMR Spectra of  $[\text{Ru}(\text{TPTTP})\text{Cl}_2]$

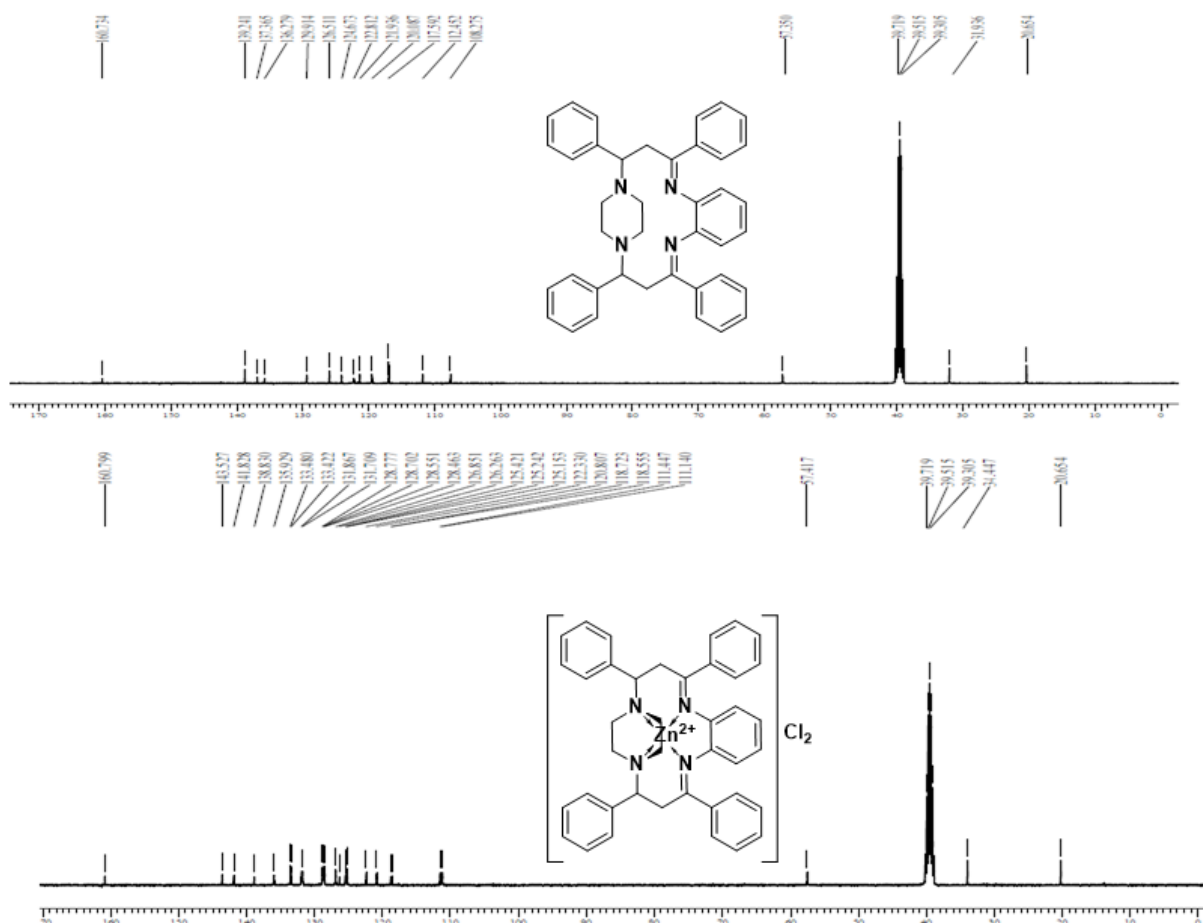


Fig. 7  $^{13}\text{C}$ -NMR Spectra of  $[\text{Zn}(\text{TPTTP})]\text{Cl}_2$

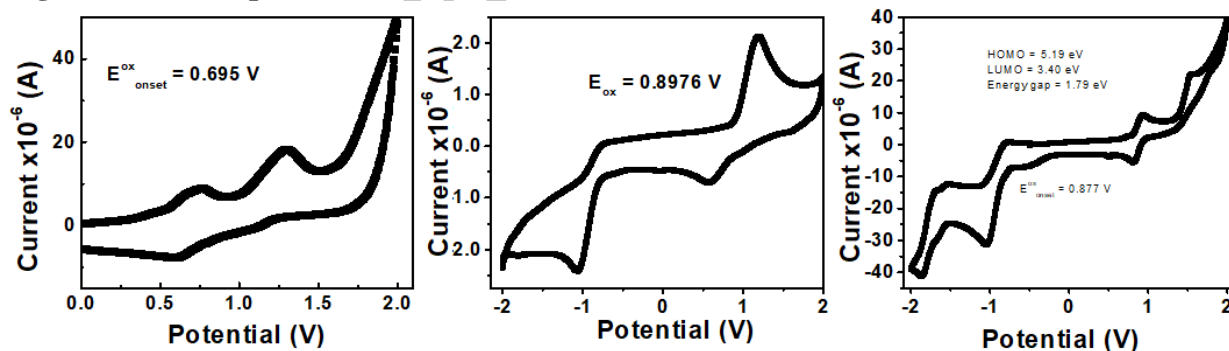
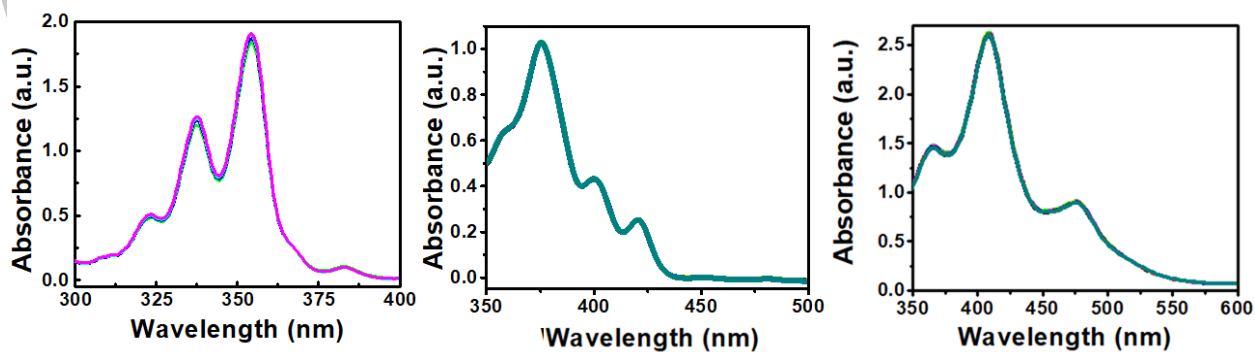
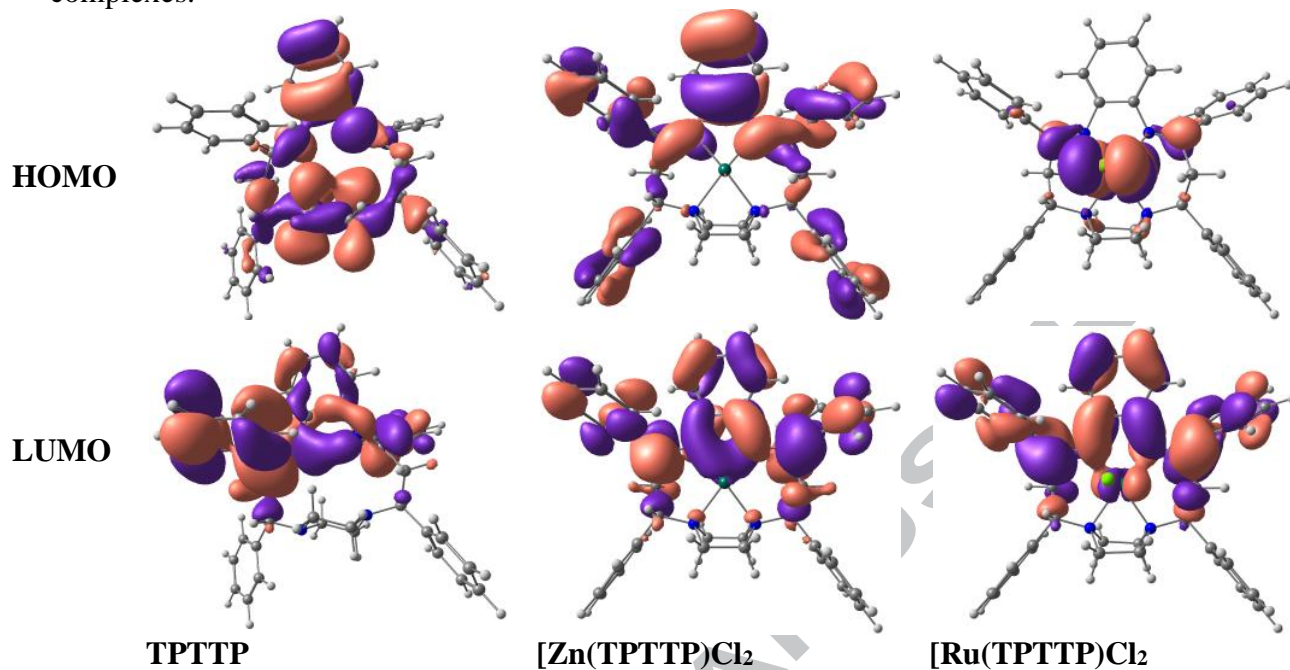


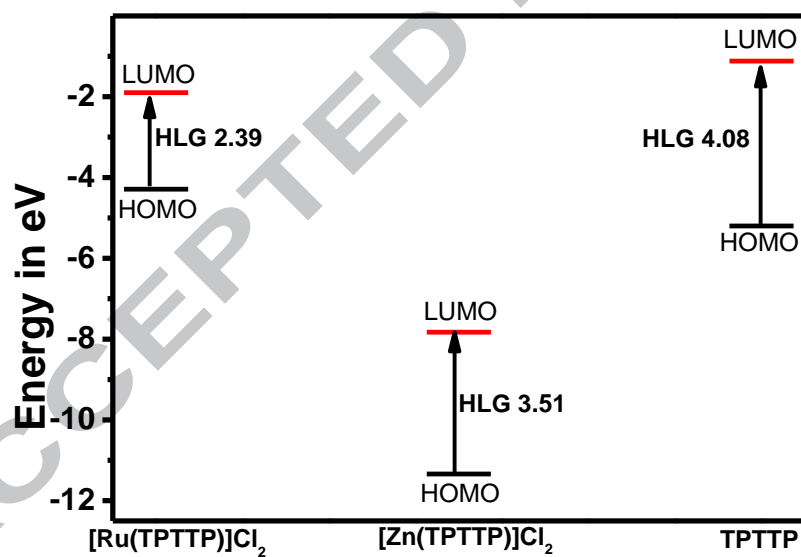
Fig. 8 Cyclic voltammograms for a) ligand, b)  $[\text{Zn}(\text{TPTTP})]\text{Cl}_2$  and c)  $\text{Ru}(\text{TPTTP})\text{Cl}_2$  of complexes.



**Fig. 9** Electronic spectra of a) ligand; b)  $[\text{Zn}(\text{TPTTP})\text{Cl}_2$  and c)  $\text{Ru}(\text{TPTTP})\text{Cl}_2$  of complexes.



**Fig. 10** HOMO-LUMO images of TPTTP,  $[\text{Zn}(\text{TPTTP})\text{Cl}_2$  and  $\text{Ru}(\text{TPTTP})\text{Cl}_2$ .



**Fig. 11** Graphical representation of HOMO-LUMO bandgap energies of TPTTP,  $[\text{Zn}(\text{TPTTP})\text{Cl}_2$  and  $\text{Ru}(\text{TPTTP})\text{Cl}_2$

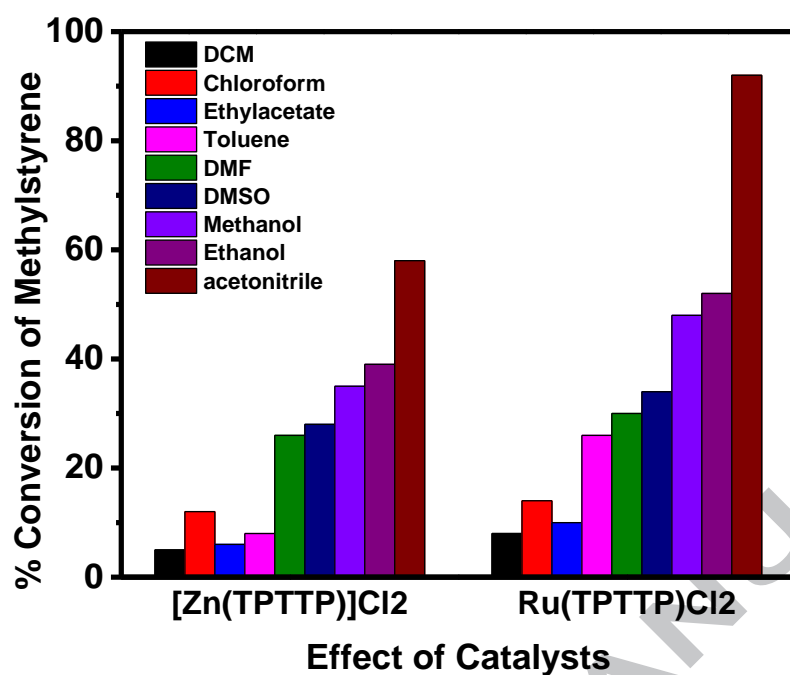


Fig. 12 Effect of solvent and their rate of conversion under visible light irradiation.

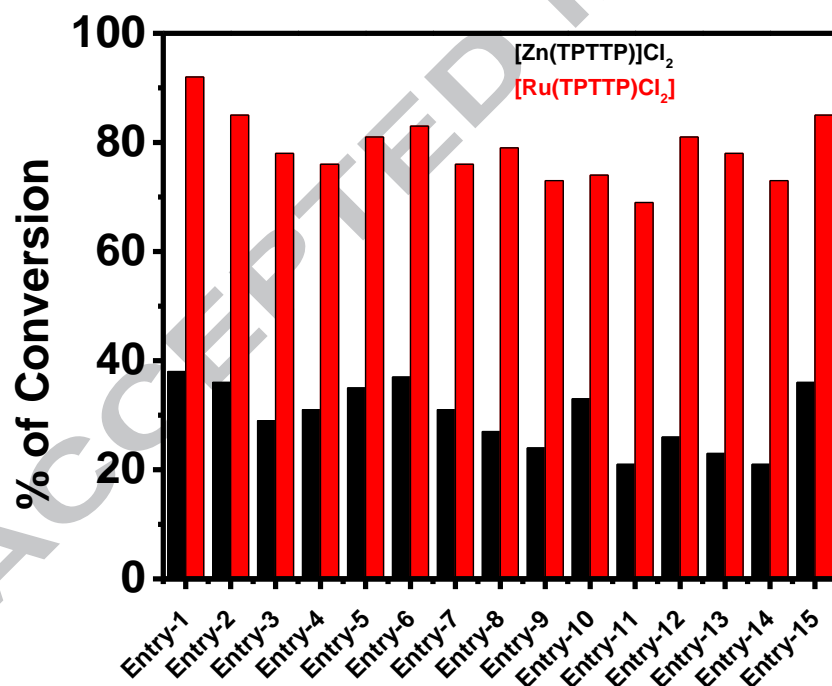
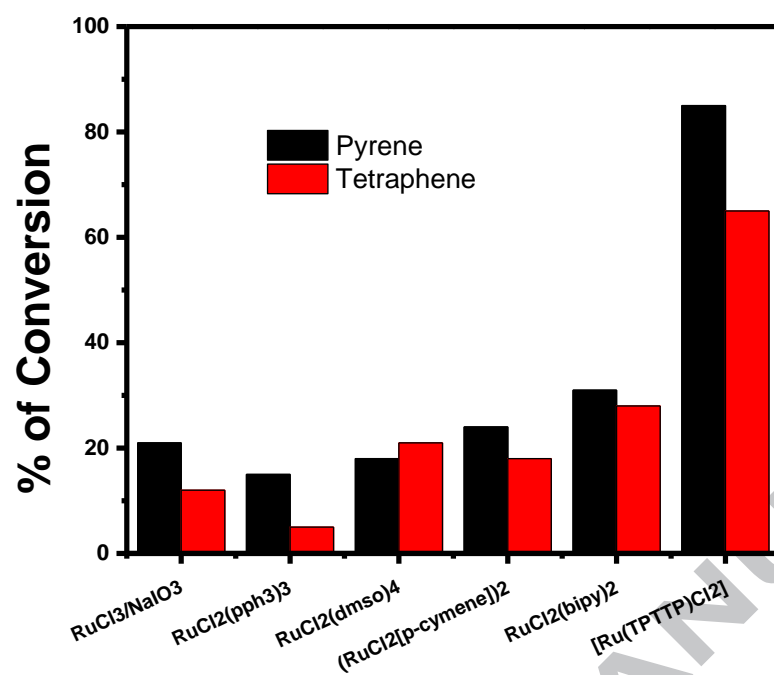
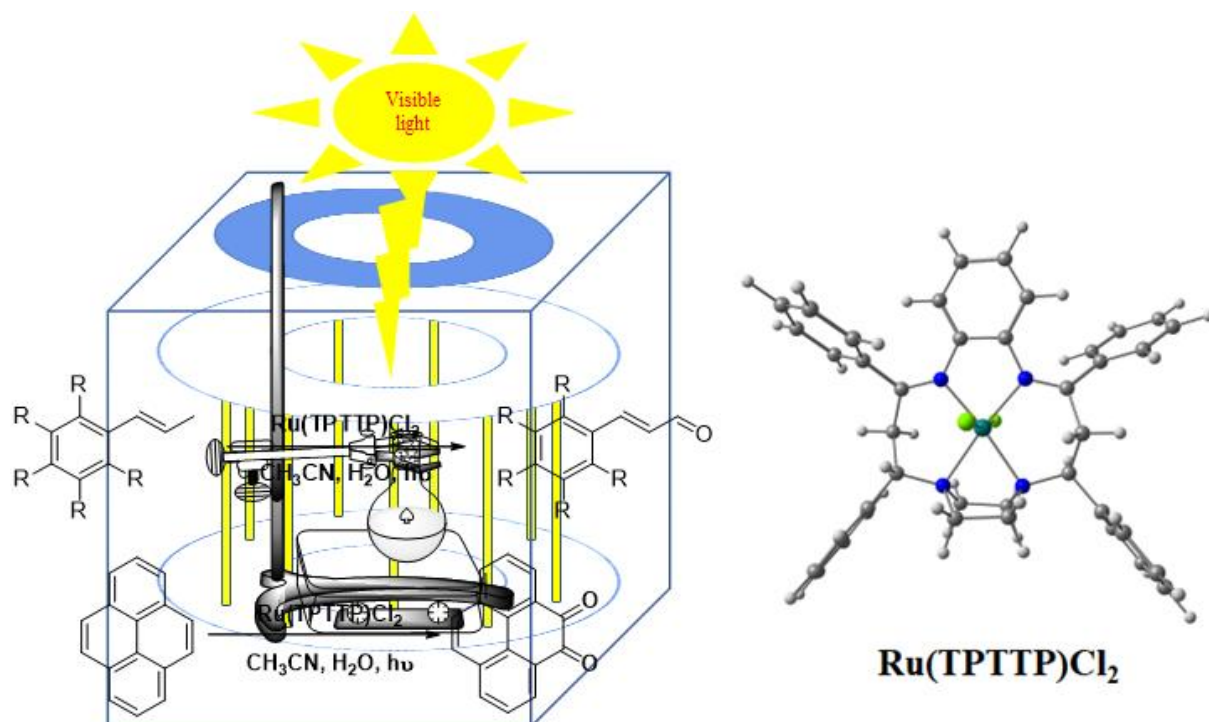


Fig. 13 Effect of complex on rate of conversion each reactant under visible light irradiation.



**Fig. 14** Optimization reaction conditions in the presence of various catalytic system under visible light irradiation.



Synthesis and characterization of new  $[\text{Zn(TPTTP)}]\text{Cl}_2$  and  $\text{Ru(TPTTP)Cl}_2$  and their photocatalytic activity studies through C-H bond activation ( $\text{sp}^3$  and  $\text{sp}^2$ ) under visible light irradiation.